*METALS AND MATERIALS International, Vol. 8, No. 5 (2002), pp. 435~441*

# Effect of Heat Treatment on Formability in 0.15C-1.5Si-1.5Mn Multiphase Cold-Rolled Steel Sheet

**Chang Gil Lee, Sung-Joon Kim, Byung-Hwan Song*, and Sunghak Lee****

Materials Processing Department, Korea Institute of Machinery and Materials
66 Sangnam-dong, Changwon 641-010, Korea
*R & D Center, Taegu Tec Corporation
304 Yonggye-ri, Gachang-myeon, Dalseong-gun, Daegu 711-860, Korea
**Center for Advanced Aerospace Materials, Pohang University of Science and Technology
San 31 Hyoja-dong, Nam-gu, Pohang 790-784, Korea

The effects of volume fraction and the stability of retained austenite on the formability of a 0.15C-1.5Si-1.5Mn (hereafter all in wt.%) TRIP-aided multiphase cold-rolled steel sheet were investigated after various heat treatments. The steel sheets were intercritically annealed at 800°C, and isothermally treated at 400°C and 430°C. Microstructural observation, tensile tests and limiting dome height (LDH) tests were conducted on the heat-treated sheet specimens, and the changes in retained austenite volume fraction as a function of tensile strain were measured using an X-ray diffractometer. The results showed a plausible relationship between formability and retained austenite stability. Although the same amount of retained austenite was obtained after isothermal holding at different temperatures, better formability was obtained in the specimens with the higher stability of retained austenite. If the stability of the retained austenite is high, the strain-induced transformation of retained austenite to martensite can be stably progressed, resulting in a delay of necking to the high strain region and improvement in formability.

**Keywords :** multi-phase cold-rolled steel sheet, TRIP, retained austenite, stability, formability

## 1. INTRODUCTION

Reduction in the weight of automobile bodies has been continuously needed in order to improve fuel efficiency and reduce the amount of emission gas for better environmental preservation. These efforts have led to rapidly rising demands for high-strength cold-rolled steel sheets with excellent formability [1]. In response to this trend, C-Si-Mn TRIP (transformation induced plasticity)-aided cold-rolled steel sheets whose microstructures are composed of ferrite, bainite, and retained austenite, have been developed [2-5]. Since they have at once both high strength and elongation because of the martensitic transformation of retained austenite during plastic deformation, they have been receiving increased attention as new high-formability cold-rolled steel sheets for automobile bodies. Studies on currently available C-Si-Mn TRIP-aided cold-rolled steel sheets reveal that most research has been mainly undertaken in the carbon content range from 0.2 to 0.4 wt.% in order to achieve a high amount of retained austenite by studying the effect of heat treatment [6,7], alloying elements [2,8,9], the transformation kinetics of retained austenite during deformation [10,11], and the deformation temperature of TRIP behavior [12,13].

Using a stretch forming test, Matsumura *et al.* [6] confirmed that the press formability of multiphase steel sheets could be improved owing to the merits of their TRIP effect, and that the initial volume fraction of retained austenite and the deformation induced transformation rate were the most important factors determining formability. Hiwatashi *et al.* [7] reported that TRIP-aided multiphase steel sheets were found to have very good stretchability near the plane-strain state and to yield high and deep drawability in the limiting dome height test. Since deformation on the punch shoulder occurs in the plane-strain state, the TRIP effect increases the fracture strength, thereby improving the deep drawability of the steel. However, despite the generally accepted knowledge of the excellent formability of TRIP-aided multiphase steel sheets due to the high strength and elongation, studies on the effect of heat treatment conditions on formability have been quite limited.

Thus, in the present study, a 0.15C-1.5Si-1.5Mn TRIP-aided multiphase cold-rolled steel sheet having lower carbon content than conventional TRIP-aided steel sheets was adopted to study the effect of heat treatment on formability. Based on the results

**Table 1.** Chemical composition (wt.%) and $A_{C1}$, $A_{C3}$, and martensite start (Ms) temperatures (°C) calculated from Andrew's equation [16] of the cold-rolled steel sheet used in this study

| C | Si | Mn | Cu | P | S | Al | $A_{C1}$ | $A_{C3}$ | Ms |
|---|---|---|---|---|---|---|---|---|---|
| 0.15 | 1.48 | 1.52 | 0.51 | 0.0016 | 0.0036 | 0.046 | 750 | 912 | 450 |

of both former studies [14,15] and present findings, the effect of the volume fractions and stability of retained austenite on mechanical properties and formability were investigated.

## 2. EXPERIMENTAL PROCEDURES

### 2.1. Preparation of cold-rolled steel sheet

A 0.15C-1.5Si-1.5Mn steel ingot was fabricated with vacuum induction melting and aluminum-killing. Table 1 lists its chemical composition, together with the $A_{C1}$, $A_{C3}$, and martensite start (Ms) temperatures calculated from Andrew's equation [16]. The steel ingot was rough-rolled into a slab 25 mm in thickness. The slab was homogenized at 1250°C for 2 hr and hot-rolled into sheets 3 mm in thickness. The hot-rolled steel sheet was pickled by a 10% HCl solution of 80°C, and was cold-rolled into sheets 0.8 mm in thickness.

Intercritical annealing was conducted for 5 min at 800°C where the volume fraction ratios of ferrite and austenite are about 50:50. Then, isothermal treatment was carried out for 3 min at 400°C (named as ECO-A) and at 430°C (named as ECO-B) followed by air cooling.

### 2.2. Microstructural observation and tensile test

The heat-treated specimens were etched in a 10% sodium metabisulfite solution ($Na_2S_2O_3 \cdot H_2O$ 10 g+$H_2O$ 100 ml), and observed with an optical microscope. Mechanical properties were evaluated by conducting tensile tests on tensile specimens (longitudinal direction) with a gauge length of 25 mm and a width of 6.3 mm. The tensile specimens were deformed at room temperature at a crosshead speed of 2.5 mm/min. using a tensile tester. The engineering stress-strain curves obtained from the tensile test were converted to true stress-true strain curves to determine the strain hardening exponent, $n$, in the uniform strain range from 5 to 20%. After the tensile specimens prepared at angles of 0°, 45°, and 90° from the rolling direction were deformed at 15%, the length and width of the gauge section before and after the deformation were measured to obtain the plastic strain ratio, $r$.

$$r = \varepsilon_0/\varepsilon_f = \ln(w_0/w_f) / \ln(t_0/t_f) \quad (1)$$

Here, $w$ and $t$ refer to the width and the thickness of the gauge section, respectively, while the subscripts 0 and f refer to pre- and post-deformation, respectively.

### 2.3. Measurement of volume fraction and stability of retained austenite

Changes in volume fraction of retrained austenite *vs* tensile strain were measured using an X-ray diffractometer (XRD). An Mo-$K_\alpha$ characteristic ray was used, and the volume fraction of retained austenite, $V_\gamma$, was calculated from the integrated intensity of the ferrite and austenite peaks using the following equation [17],

$$V_\gamma = 1.4I_\gamma/(I_\alpha + 1.4I_\gamma) \quad (2)$$

where $I_\gamma$ is the average integrated intensity obtained at the $(220)_\gamma$ and $(311)_\gamma$ peaks, and $I_\alpha$ is that obtained at the $(211)_\alpha$ peak.

To evaluate the stability of retained austenite as a function of heat-treatment, the strain-induced martensitic transformation rate formula, recently suggested by Chung [10] and Chang *et al.* [11], was applied.

$$\log [\ln f_s / (f_s - f)] = \log\kappa + m\log\varepsilon \quad (3)$$

Here, $f_s$ and $f$ refer to the saturated martensite volume fraction and the martensite volume fraction transformed during deformation, respectively, while ε and $m$ refer to the true strain and the deformation mode coefficient, respectively. κ is defined as the stability coefficient of retained austenite, and the larger κ value indicates the lower stability of retained austenite and the faster martensitic transformation.

### 2.4. Evaluation of formability

To evaluate the stretch formability of the cold-rolled steel sheet specimens as a function of heat-treatment, limiting dome height (LDH) tests were conducted using a hemispheric punch. A schematic diagram of the LDH test is given in Fig. 1. The minimum limiting dome height, *LDHo*, was obtained from 180-mm-long rectangular specimens of varying width. The rectangular specimens were marked on the surface with

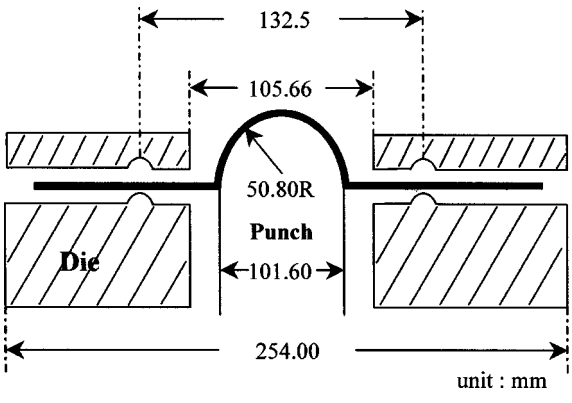


**Fig. 1.** Schematic diagram of the limiting dome height (LDH) test.

circular grids using the electro-chemical etching method, and were deformed until either local necking or fracture occurred. Upon punching, the circular grids were changed into an oval shape. The forming limit curve (FLC) was drawn by measuring major strain ($\varepsilon_1$) and minor strain ($\varepsilon_2$) together with the strains of the locally necked region and the un-necked region, using an optical grid analyzer after the limit strain was established.

## 3. RESULTS

### 3.1. Microstructure

Figs. 2(a) and (b) are optical micrographs of the two heat-treated steel sheet specimens after they were etched in a sodium metabisulfite solution. When the etched specimens are observed with an optical microscope, it is easier to define the phases since ferrite is displayed as gray, bainite or martensite as black, while retained austenite as white [5]. The volume fractions of retained austenite are about 11% in both specimens. Retained austenites are homogeneously distributed throughout the microstructure, and are mostly connected with adjacent ferrites or bainites. Based on *in situ* TEM deformation test results to study the relationship between the shape of retained austenite and the strain-induced martensite transformation, Chung [10] reported that only those retained austenites connected with adjacent ferrites or bainites are transformed to martensites during plastic deformation, and thus contribute to enhanced ductility, whereas film-type austenites located between bainite laths and austenites isolated inside ferrite grains are not transformed to martensites even though a considerable amount of plastic deformation is applied.

### 3.2. Tensile properties

Tensile specimens angled at 0°, 45°, and 90° from the rolling direction were tested, and the results are given in Table 2. The tensile properties of neither specimen varied much, although the ECO-A shows a little lower strength and higher elongation than the ECO-B. Tensile elongation was around 30%, despite the high tensile strength above 720 MPa. The strain hardening exponent, *n*, was almost the same regardless of heat-treatment conditions. The plastic strain ratio, *r*, also did not fluctuate much, and stayed around 0.91~0.96. Although the uniform strain stays around about the same level, the ECO-A specimen isothermally treated at 400°C shows slightly higher value than the ECO-B specimen isothermally treated at 430°C.

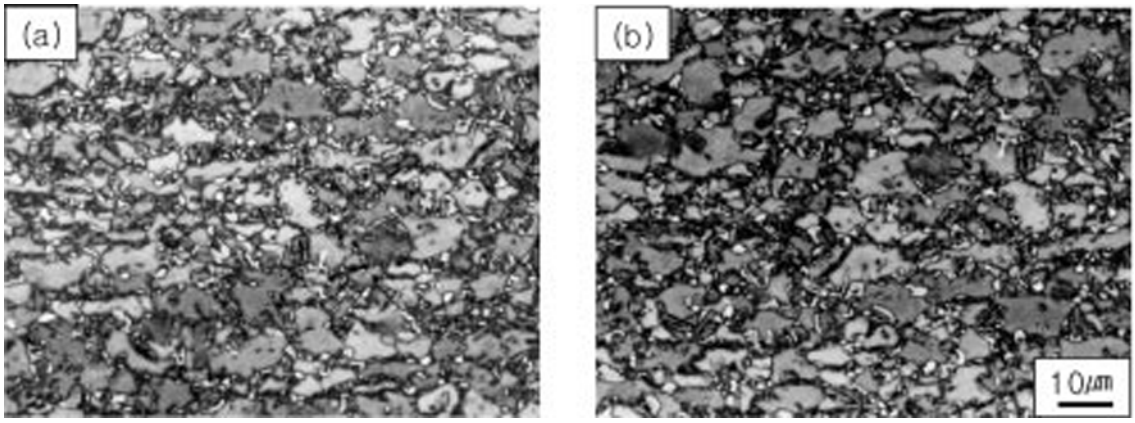


**Fig. 2.** Optical micrographs of the (a) ECO-A, and (b) ECO-B specimens. Etched with 10% sodium metabisulfite solution.

**Table 2.** Mechanical properties of ECO-A and ECO-B specimens

| Specimen | Angle to Rolling Direction | Yield Strength (MPa) | Tensile Strength (MPa) | Elong. (%) | Uniform Elong. (%) | n | r |
|---|---|---|---|---|---|---|---|
| ECO-A | 0° | 455.1 | 716.3 | 33.74 | 28.73 | 0.264 | 0.877 |
| | 45° | 463.9 | 719.4 | 32.38 | 26.88 | 0.268 | 0.855 |
| | 90° | 463.9 | 726.5 | 33.49 | 27.55 | 0.261 | 1.065 |
| | Mean* | 461.7 | 720.4 | 33.00 | 27.51 | 0.265 | 0.913 |
| ECO-B | 0° | 455.3 | 733.1 | 35.14 | 29.56 | 0.247 | 1.07 |
| | 45° | 471.6 | 723.2 | 27.61 | 23.12 | 0.266 | 0.86 |
| | 90° | 476.6 | 728.9 | 26.49 | 23.52 | 0.278 | 1.04 |
| | Mean* | 468.8 | 727.1 | 29.21 | 24.83 | 0.264 | 0.96 |

*Mean value, $X = (X_0+2X_{45}+X_{90})/4$

**Table 3.** Chemical compositions and mechanical properties of steel sheets for purpose of comparison with ECO-A and ECO-B specimens [7,18]

| steel | Composition (wt.%) | | | | | n | r | Mechanical Properties | | | |
|---|---|---|---|---|---|---|---|---|---|---|---|
| | C | Mn | Si | P | S | | | T.S.(MPa) | Y.S.(MPa) | TEl.(%) | UEl.(%) |
| P | 0.13 | 1.35 | 0.25 | 0.018 | 0.002 | 0.172 | 0.88 | 564 | 431 | 27.5 | 16.9 |
| D | 0.09 | 2.07 | 0.03 | 0.025 | 0.006 | 0.185 | 0.70 | 653 | 346 | 27.0 | 18.4 |
| S | 0.09 | 0.19 | 0.99 | 0.016 | 0.006 | 0.188 | 0.87 | 343 | 323 | 35.7 | 22.0 |

In order to compare the results with the well-known high formability steel sheets, the results studied by Hiwatashi *et al.* [7,18] are given in Table 3. In the table, P indicates an equivalent-strength precipitation-hardened steel, D a ferrite/martensite dual-phase steel, and S an equivalent-elongation phosphorus solid solution-hardened steel. Compared with the results given in the Tables 2 and 3, it may be seen that, in spite of the high strength the ECO-A and B steels, they show higher elongation than steels P and D having a strength of 500~600 MPa and similar elongation to the steel S having lower strength. The plastic strain ratio ($r$) and strain hardening exponent ($n$) of the ECO-A and B steels are larger than those of the P, D, and S steels.

Fig. 3 shows the changes in the strain hardening exponent as a function of true strain obtained from the log (true stress) log (true strain) curve of every steel mentioned above. The strain hardening exponents of the P, D, and S steels decrease continuously as the true strain increases, whereas the higher exponents of the ECO-A and B are maintained almost constant up to 25% of true strain. This finding results from the delay in necking to higher strain owing to the strain-induced martensite transformation of retained austenite [19,20].

### 3.3. Formability of the multiphase steel sheets

The limiting dome heights (*LDHo*) of the ECO-A and B steels are 37.1 and 35.2 mm, respectively, and the *LDHo* of the S, P, and D steels are 24~28 mm [18]. LDH in general has a minimum value depending on the specimen width [21]. The minimum value in the cold-rolled steel sheets for automobiles exists somewhere between 126 mm and 132 mm, and the higher value indicates better formability in the stamping process. Meanwhile, the *LDHo*, which is a measurement of stamping formability, is generally known to be linearly proportional to the uniform strain under uniaxial tension [22]. The ECO-A shows higher uniform strain and *LDHo* than the ECO-B, indicating that the formability is greatly affected by the stability of retained austenite in spite of the similar initial volume fraction of their retained austenite.

Fig. 4 shows the forming limit curves (FLCs) obtained from the measurements of the deformed circular grids with an optical grid analyzer. In general, the higher the FLC level the better the formability. The *FLCo* value, which is the limit plane strain corresponding to the lowest point in a plane

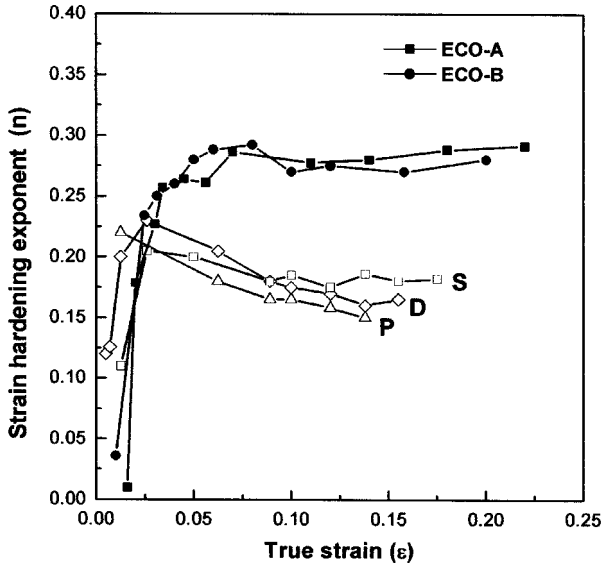


**Fig. 3.** Strain hardening exponent, $n$, as a function of true strain of the ECO-A and ECO-B specimens compared with conventional steel sheets.

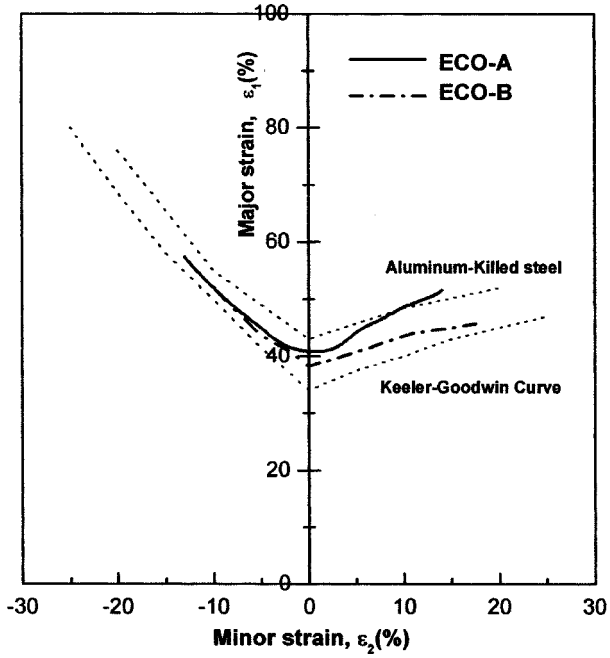


**Fig. 4.** Forming limit curves of ECO-A and ECO-B specimens obtained from measurements of deformed circular grids with an optical grid analyzer.

strain mode ($-0.1<\varepsilon_2<0.2$), indicates the level of forming performance [22-24]. Although the *FLCo* values of both steels are a little lower than that of aluminum-killed cold-rolled steels [25], the pattern of the curves is similar. Comparing Fig. 4 and Table 2, it may be seen that the *FLCo* of the ECO-A is higher by about 5% than that of ECO-B, since ECO-A has a higher elongation in spite of their similar strain hardening exponent. In addition, the FLCs of both steels lie in between the Keeler-Goodwin band [26], indicating that the overall formability of both steels is superior or similar to the formability of commercial low carbon cold-rolled steels.

### 3.4. Stability of retained austenite

The volume fraction changes of retained austenite as a function of tensile strain in the ECO-A and B steels measured by XRD are given in Fig. 5. The initial volume fraction of both steels is around 11%, and the strain-induced transformation of both specimens behaves quite similarly. The amount of retained austenite drastically decreases until the strain reaches about 0.1, and then the reduction rate decreases slowly. The volume fraction of retained austenite in ECO-A is higher than that of ECO-B when the true strain is same. Thus, the resistance to deformation from retained austenite to martensite is larger in ECO-A than in ECO-B.

The results of Fig. 6 were applied to Eq. 3, and the resulting interpretation was displayed in Fig. 6. 74.8% of the initial retained austenite in the ECO-A specimen was transformed to martensite during tensile deformation prior to necking, while 78.9% in the ECO-B specimen. The slope of straight lines, *m*, in Fig. 6 and Eq. 3, being the deformation mode coefficient, is reported to stay stable at 1.0 in C-Si-Mn TRIP-aided cold-rolled steel sheets composed of ferrite, bainite, and

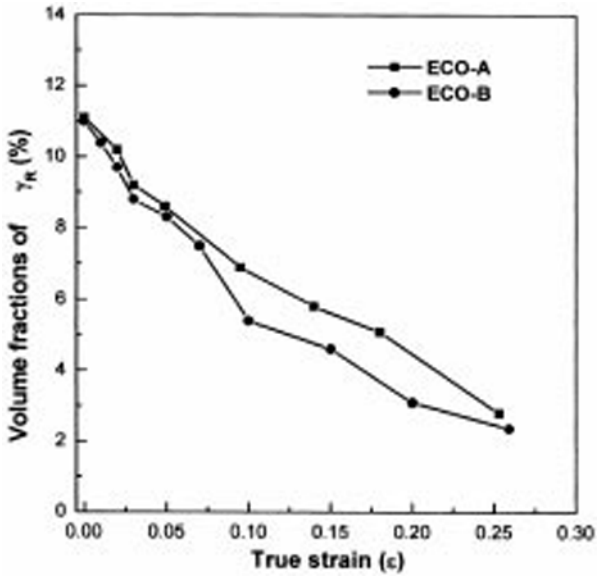


**Fig. 5.** Volume fraction changes of retained austenite as a function of true strain.

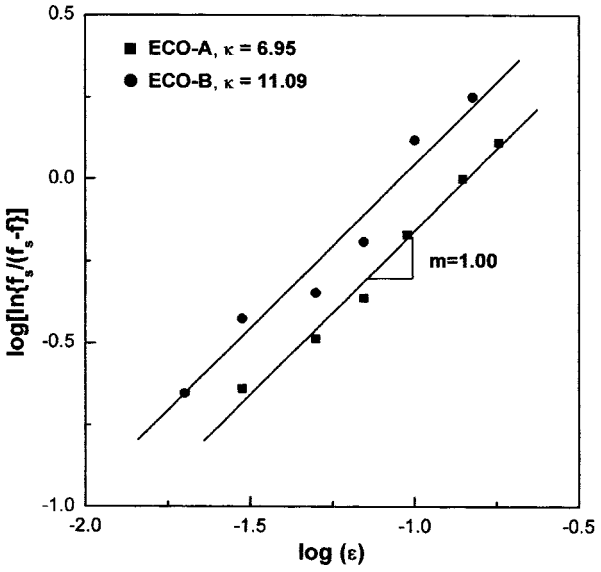


**Fig. 6.** Relationship between $\log[\ln f_s/(f_s-f)]$ and loge. The deformation mode coefficient as represented by the slope, *m*, is near 1.0.

retained austenite, regardless of the heat-treatment condition [10]. In general, lower *k* value indicates the higher stability of retained austenite [11]. The ECO-A specimen shows the lower κ of 6.63 compared with that of the ECO-B, 10.76, indicating that the stability of retained austenite in the ECO-A is higher than that of ECO-B and that the strain induced martensite transformation is more delayed in ECO-A when the same amount of deformation is induced. This stability of retained austenite is closely related with the mechanical properties of cold-rolled steel sheets, with uniform elongation in particular. This is because necking is delayed as the strain-induced transformation lasts up to the higher strain region when the stability of retained austenite is high.

## 4. DISCUSSION

In developing multiphase cold-rolled steels, the optimum intercritical annealing and isothermal heat treatment to obtain a larger amount of retained austenite with higher stability results in the best combination of high strength and high ductility. Also, it is necessary to evaluate the formability of cold-rolled steel sheet and to analyze the effect of retained austenite on formability. In this study, the formability of 0.15C-1.5Mn-1.5Si TRIP-aided multiphase steel is compared with commercial grade high formability steels, and discussed in consideration of the stability of retained austenite.

The plastic strain ratio, *r*, and strain hardening exponent, *n*, are predominantly used for evaluating the formability of sheet metal. Whiteley [27] verified that the increase in *r* led to the increase in the limiting drawing ratio in deep drawing tests. Keeler and Beckofen [28] also reported that the increase in *n* led to homogeneous strain distribution and improved

stamping formability. The *LDHo* of the ECO-A and B steels is higher by 10~15 mm than those of conventional high-formability cold-rolled steel sheets, meaning that the formability of ECO-A and B is superior to that of P, D, and S steels. This can be attributed to the fact that the ECO-A and B specimens have a higher strain hardening exponent maintained to high strain, as shown in Fig. 3. The high strain hardening exponent and excellent formability of multiphase steels are due to the strain-induced transformation of retained austenite and large uniform elongation. When ferrite, bainite, and retained austenite are coexisting, ferrite undergoes strain hardening, and strain energy is accumulated by dislocation pile-up inside ferrite grains. The accumulated strain energy provides the mechanical driving force needed for the strain-induced transformation of retained austenite [29]. Upon strain-induced martensite transformation, this energy is absorbed, dislocation pile-up is relaxed, and the ferrite grains are softened. The softened ferrite grains are strain-hardened again by the transformed martensite. This process is repeated throughout the process of the strain-induced martensite transformation of retained austenite. If the stability of retained austenite is high, the strain-induced martensite transformation can proceed steadily even under high strain, and thus can enhance formability because the abrupt drop in strain hardenability can be prevented. Therefore, the stability of retained austenite is an important factor directly affecting formability.

ECO-A and B have similar tensile properties such as yield strength, tensile strength, strain hardening exponent, and plastic strain ratio excepting uniform and tensile elongation, as given in Table 2. However, the *LDHo* and *FLCo* of the ECO-A are higher than those of ECO-B. This results from the higher stability of retained austenite in ECO-A. Fig. 5 shows the higher volume fraction of retained austenite in ECO-A compared with ECO-B when the true strain is the same, and the stability coefficient, $\kappa$, interpreted from Changs equation [11] is also lower than that of ECO-B, as shown in Fig. 6. This means that the flow stress of ECO-A has to be higher than that of ECO-B, if the same amount of retained austenite is transformed to martensite. The higher stability, *i.e.* the lower $\kappa$, contributes to the resistance of retained austenite to deformation, and delays the local necking up to the high strain region. Thus, ECO-A steel can be considered to have higher uniform elongation and more excellent formability than ECO-B steel.

As mentioned above, the stability as well as the volume fraction of retained austenite is a very important factor determining mechanical properties and formability. The most important factor affecting the stability of retained austenite is carbon content. When the overall chemical compositions of cold-rolled steels are the same, the carbon content of retained austenite is determined by the heat treatment condition, *i.e.* intercritical annealing and isothermal treatment. In the case of the ECO-A and B steels, the annealing temperature was selected as 800°C at which the volume fraction ratio of ferrite and austenite is 50:50, since the most excellent tensile strength and elongation can be obtained [14,15]. Considering the phase transformation during the isothermal treatment, only the austenite formed during annealing is transformed to bainite. Since almost all the carbons are dissolved in the austenite, the Ms (martensite starting) temperature of the austenite formed during intercritical annealing is lower than the Ms temperature of cold-rolled steel sheet itself. If the solubility of carbon in ferrite can be ignored, the carbon content of austenite becomes 0.32%. The Ms temperature of the austenite calculated from Andrews equation [16] is around 370°C, although the Ms temperature of the whole steel sheet is around 430°C. According to previous research [10,14], the optimum isothermal heat treatment temperature is Ms+20~30 to give the best combination of high strength and ductility. Based on these results, 400°C was selected as the isothermal temperature for ECO-A steel, whereas the isothermal heat treatment temperature for ECO-B steel was 430°C which is Ms+60°C. Although the initial volume fractions of retained austenite are the same in ECO-A and B steels, the stability of retained austenite is different in those steels. This difference of stability results in the difference in formability in spite of their similar tensile strength and elongation. Also, the difference in stability between ECO-A and B steels results from the difference in isothermal heat treatment temperature. Therefore, in consideration of the stability of retained austenite, the isothermal heat treatment temperature should be determined based on the chemical composition of the austenite formed during intercritical annealing.

## 5. CONCLUSIONS

In the present study, a 0.15C-1.5Si-1.5Mn TRIP-aided multiphase cold-rolled steel sheet was fabricated, and its tensile properties and formability were evaluated and compared with commercial grade cold-rolled steel sheets. The following conclusions were reached:

1. The low-carbon TRIP-aided multiphase cold-rolled steel sheet was found to have formability superior to conventional high formability cold-rolled steels, since the multiphase steel maintained work hardenability up to a high strain range owing to the TRIP effect.

2. The mechanical properties and formability of multiphase steels are largely determined by the stability of retained austenite, when the volume fractions of retained austenite are the same.

3. Heat treatment conditions should be established in such a way as to promote higher stability as well as higher volume fraction of retained austenite in order to improve the formability of TRIP-aided multiphase cold-rolled steel sheets while taking into consideration the chemical composition of the austenite formed during intercritical annealing.

## ACKNOWLEDGMENT

This work was financially supported by the Ministry of Science and Technology of Korea, under the National Research Laboratory program.

## REFERENCES

1. H. Hayashi, *CAMP-ISIJ* **11**, 388 (1993).
2. K. Sugimoto, N. Usui, M. Kobayashi, and S. I. Hashimoto, *ISIJ Int*. **32**, 1311 (1992).
3. K. Sugimoto, M. Kobayashi, and S. I. Hashimoto, *Metall. Trans. A* **23**, 3085 (1992).
4. H. C. Chen, H. Era, and M. Shimizu, *Metall. Trans. A* **20**, 437 (1989).
5. C. G. Lee and S. J. Kim, *J. Kor. Inst. Met. & Mater*. **36**, 1024 (1998).
6. O. Matsumra, Y. Sakuma, Y. Ishii, and J. Zhao, *ISIJ Int*. **32**, 1110 (1992).
7. S. Hiwatashi, M. Takahashi, T. Katayama, and M. Usuda, *J. Jpn. Soc. Tech. Plasticity* **35**, 1109 (1994).
8. K. Sugimoto, M. Kobayashi, A. Nagasaka, and S. Hashimoto, *ISIJ Int*. **35**, 1407 (1995).
9. N. C. Goel, S. Sangal, and K. Tangri, *Metall. Trans. A* **16**, 2013 (1985).
10. J. H. Chung, *Ph. D. Thesis*, POSTECH (1993).
11. H. C. Shin, T. K. Ha, and Y. W. Chang, *J. Kor. Inst. Met. & Mater*. **34**, 1550 (1996).
12. K. Imai, M. Komatsu, and W. Kokuju, *CAMP-ISIJ* **6**, 754 (1993).
13. K. Sugimoto, M. Kobayashi, and S. Hashimoto, *J. Jpn. Inst. Met*. **54**, 657 (1990).
14. S. G. Park, C. G. Lee, S. J. Kim, and I. D. Choi, *J. Kor. Inst. Met. & Mater*. **36**, 1234 (1998).
15. C. G. Lee, S. J. Kim, S. G. Park, and I. D. Choi, *J. Kor. Inst. Met. & Mater*. **36**, 1382 (1998).
16. K. W. Andrew, *J. Iron Steel Inst*. **203**, 721 (1965).
17. R. L. Miller, *Trans. ASM* **61**, 592 (1968).
18. Y. Sakuma, N. Kimura, A. Itami, S. Hiwatashi, O. Kawano, and K. Sakata, *Nippon Steel Technical Report* **64**, 20 (1995).
19. J. M. Rigsbee and P. J. VanderArend, *Formable HSLA and Dual-Phase Steels* (ed., A. T. Davenport), p. 56, TMS-AIME, Warrendale, PA (1979).
20. O. Matsumura, Y. Sakuma, and H. Takechi, *Scripta metall*. **21**, 1301 (1987).
21. R. A. Ayres, *J. Appl. Met. Working* **1**, 73 (1979).
22. Y. S. Kim and K. C. Park, *J. Kor. Soc. Mech. Eng*. **33**, 47 (1993).
23. R. Sowerby and J. L. Duncan, *Int. J. Mech. Sci*. **13**, 217 (1971).
24. M. J. Painter and R. Pearce, *J. Phys. D: Appl. Phys*. **7**, 992 (1974).
25. S. P. Keeler, *Sagamore Army Materials Res. Conf*., Raquette Lake, NY (1974).
26. S. P. Keeler, *Proc. 21st Sagamore Conf*.: *Advances in Deformation Processing*, Plenum Press, NY (1978).
27. R. L. Whiteley, *Trans. ASM* **52**, 154 (1959).
28. S. P. Keeler and W. A. Backofen, *Trans. ASM* **56**, 25 (1963).
29. S. K. Kim, H. C. Shin, J. H. Chung, and Y. W. Chang, *J. Kor. Inst. Met. & Mater*. **36**, 151 (1998).